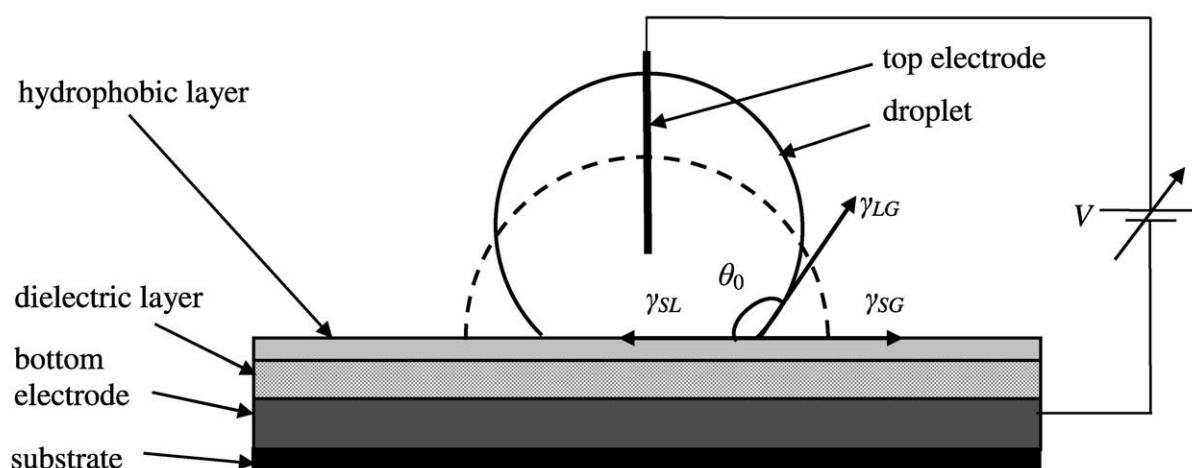
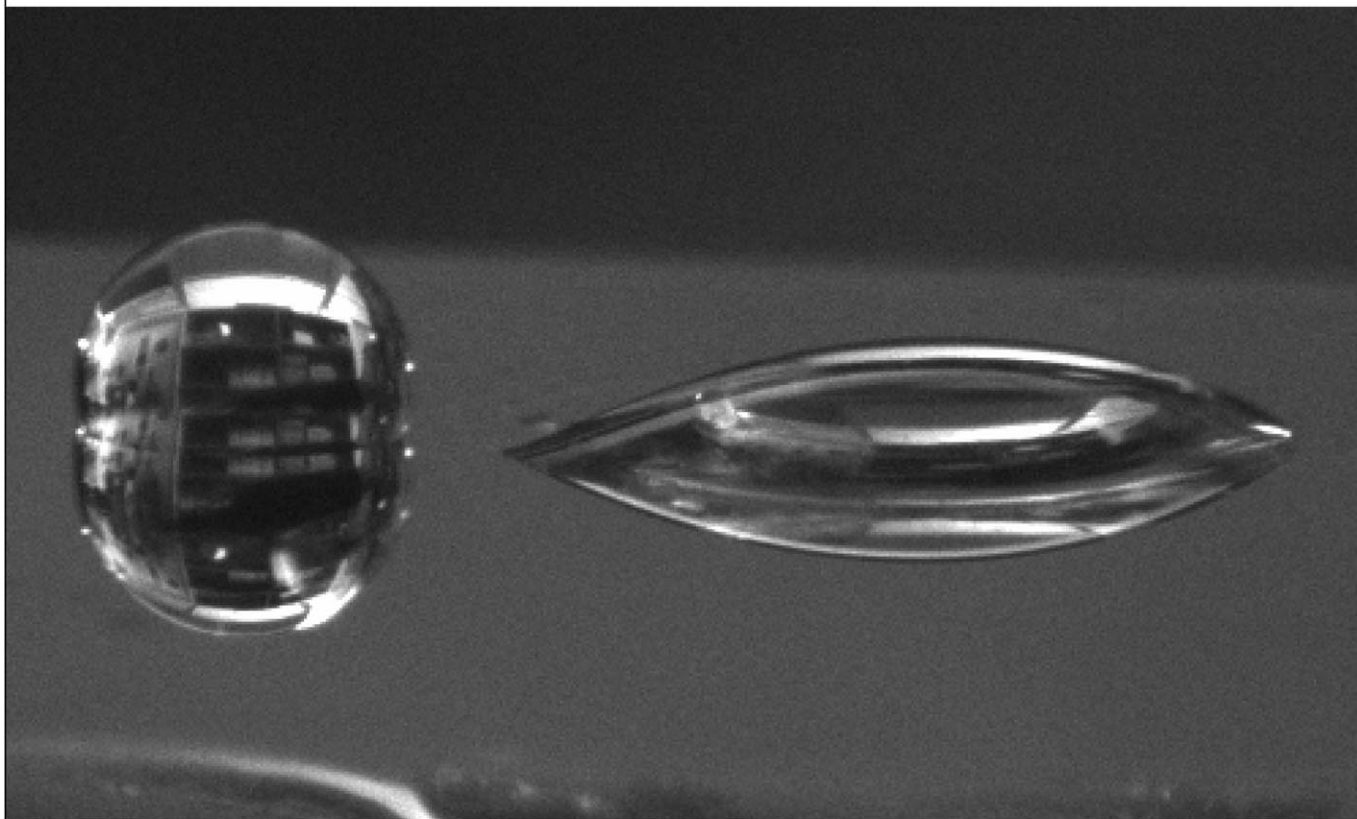


## Switchable Surfaces



# Intelligent Control of Surface Hydrophobicity

Sally L. Gras,<sup>\*,[a]</sup> Tanveer Mahmud,<sup>[b]</sup> Gary Rosengarten,<sup>[c]</sup> Arnan Mitchell,<sup>[b]</sup> and Kourosh Kalantar-zadeh<sup>[b]</sup>

*Switchable surfaces are highly useful materials with surface properties that change in response to external stimuli. These surfaces can be employed in both research and industrial applications, where the ability to actively control surface properties can be used to develop smart materials and intelligent surfaces. Herein, we review a range of surfaces in which hydrophobicity can be controlled. We present the principal ideas of surface switching, discuss recent developments, explore experimental issues and examine factors that influence surface switching, including the*

*nature of the stimuli, the underlying material, the morphology of the surface and the surrounding environment. We have categorised switchable surfaces according to the stimuli that trigger changes in surface hydrophobicity. These are electrically, electrochemically, thermally, mechanically, photo- and environmentally inducible surfaces. In addition, we review the use of chemical reactions to modify the properties of switchable surfaces and produce changes in the molecular structure and nanoscale features of the surface.*

## Introduction

The intelligent control of surface properties by external stimuli is of great importance in microsystems, materials science, biotechnology and medicine, where the responsive nature of a surface yields additional and possibly vital functionality to the material or device. The concept of switchable surfaces has raised broad scientific interest, and a substantial body of research has examined surface properties, together with methods for modifying and controlling these properties. Most studies aim to develop reversible control, in which the surface properties are altered when stimuli are applied and then regenerated when the stimuli are removed or an alternate trigger is applied. Nonreversible modification may also be desirable for some applications, such as surgical implants or disposable devices.

Herein, we focus on surfaces where external stimuli can trigger changes in surface hydrophobicity. The resulting change in surface wetting may be observed by monitoring the change in contact angle between a droplet of water or aqueous solution and the surface. Changes to surface wetting have a significant effect on surface properties and influence interfacial interactions with both aqueous and organic liquids and with gases. Moreover, these surface changes alter interactions with biomolecules, including DNA, RNA and proteins, and change the response of cells and tissues that come into contact with the surface.

Various actuation methods have been utilised to control surface hydrophobicity and surface wetting, including electrical potential, electrochemical stimuli, photoillumination, thermal energy, mechanical stress and changes to the surrounding environment, such as pH value or the presence of organic or inorganic liquids. These techniques can be employed to develop smart devices with potential applications in many fields. In microfluidics the surface area-to-volume ratio is much larger than that for macroscale systems, so that surface forces dominate.

Thus, switchable surfaces are ideal for microfluidics, and they can be used to fabricate direct pumping devices and valves with no moving mechanical parts. Such devices will be useful as microscaled chemical dispensers, injectors, reactors and integrated cooling systems for high-density microelectronics.<sup>[1]</sup> Customised surfaces can also be utilised for the fabrication of liquid micromotors<sup>[2]</sup> with unique characteristics including movement with reduced friction, which results in reduced wear on parts and low power consumption.

Switchable surfaces may be used to develop new techniques for manipulating liquids. For example, photoinduced changes in wettability can be used to control the spread of liquids on a surface and enhance the solubility of solutes at the surface/liquid interface. These properties may be exploited for coating processes and for use in microanalytical devices.<sup>[3]</sup> Potential applications are not limited to aqueous systems. The control of surface wettability at organic interfaces, such as oil droplets, could also be applied in microsystems, for example electro-optical devices and optical switches.<sup>[4]</sup>

[a] Dr. S. L. Gras  
Department of Chemical and Biomolecular Engineering and the  
Bio21 Molecular Science and Biotechnology Institute  
The University of Melbourne  
Parkville 3010 (Australia)  
Fax: (+61) 3-8344-4153  
E-mail: sgras@unimelb.edu.au

[b] T. Mahmud, Prof. A. Mitchell, Dr. K. Kalantar-zadeh  
School of Electrical and Computer Engineering  
RMIT University  
Melbourne 3000 (Australia)

[c] Dr. G. Rosengarten  
School of Mechanical and Manufacturing Engineering  
The University of New South Wales  
Sydney 2052 (Australia)

The potential of surfaces with controlled wettability has already been demonstrated in the development of programmable drug-delivery devices,<sup>[5]</sup> bioanalysis,<sup>[6]</sup> micro- and nanoscale chemical process systems<sup>[7]</sup> and protein separation.<sup>[8]</sup> It is clear that further wide-ranging applications will also be developed as the field of switchable surfaces matures and the full potential of surfaces with interchangeable properties is realised.

Herein, we review recent advances in the active control of surface properties for responsive materials that are triggered by external stimuli. The article is ordered according to the activation stimulus used to modify surfaces and to control the in-

teraction of surfaces with neighbouring liquid or gas environments.

## Electrical Switching

One method for modifying the hydrophobicity of a surface, effectively making it more hydrophilic, is to apply a static electric field. This process is called electrowetting, as the surface experiences a change in wettability. The surface tension of a polar liquid droplet in contact with the surface decreases, which results in a decrease in the contact angle between the liquid and the surface. A schematic illustration of electrowetting for a liquid/solid interface is shown in Figure 1. Such experiments require an underlying electrode to conduct the electrical energy and can include a nonconductive dielectric layer, which insulates the hydrophobic surface from the bottom electrode. An accumulation of charge at the interface or polarisation of the surface is responsible for the change in surface properties. Electrowetting may also be applied to modify the interaction between two immiscible liquids, and this type of interaction offers a further avenue for developing switchable liquid-based systems. For example, electrowetting may be used to create adjustable liquid lenses.<sup>[9]</sup>

Electrowetting can be effectively described by the Lippmann–Young<sup>[10–16]</sup> equation, which relates the contact angle  $\theta$  (after application of the voltage) to the surface tension at the

Sally Gras is a lecturer in the Department of Chemical and Biomolecular Engineering and research group leader at the Bio21 Molecular Science and Biotechnology Institute at The University of Melbourne, Australia. She received her Ph.D. from Cambridge University and her B.Sc. (Biochemistry and Molecular Biology) and B.Eng. (Chemical) degrees from The University of Melbourne. Her research interests include amyloid fibrils, the design and development of novel materials and cell–material interactions.



Tanveer Mahmud is a Ph.D. candidate at RMIT University, Melbourne, Australia and works in optofluidics. He has completed his Masters of Engineering in Microelectronic Engineering from RMIT University, Australia, and Bachelor of Science in Electrical and Electronic Engineering from the Islamic University of Technology, Dhaka, Bangladesh. His research interests are optofluidics, microfluidic devices and electrically wettable surfaces.



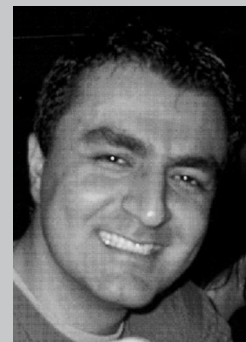
Gary Rosengarten is a senior lecturer in the School of Mechanical and Manufacturing Engineering at the University of New South Wales, Australia, where he heads the microfluidics and heat transfer groups. He completed honours degrees in Physics and Mechanical Engineering at Monash University, and a Ph.D. at the University of NSW. His research interests include fluid flow and heat transfer for micro- and nanosystems specifically related to biomedical devices and to energy systems, surface effects in microfluidics, and integrated sensors for lab-on-a-chip.



Arnan Mitchell is Associate Professor of Photonics in the School of Electrical and Computer Engineering and research manager of the Microelectronics and Materials Technology Centre (MMTC) at RMIT University, Australia. He received his Ph.D. from RMIT University and his Bachelor of Technology (Optoelectronics) degree from Macquarie University, Australia. His research interests include electro-optic nonlinear waveguide photonics and micro- and nanofabrication with particular interest in the emerging area of optofluidics.



Kourosh Kalantar-zadeh is a senior lecturer at the School of Electrical and Computer Engineering, RMIT University, Australia. He received his B.Sc. and M.Sc. from Sharif University of Technology, Iran, and Tehran University, Iran, respectively, and completed his Ph.D. at RMIT University, Australia. His research interests include chemical and biochemical sensors, nanotechnology, microsystems, materials science, electronic circuits and microfluidics.



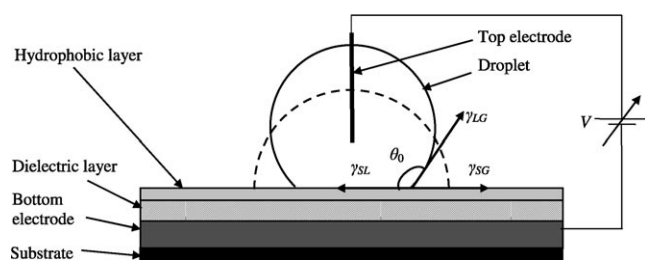


**Figure 1.** Schematic illustration of electrowetting: the solid and dashed lines show the droplet shape prior to and following the application of an applied voltage, respectively.  $\theta_0$  is the water contact angle when the applied voltage across the electrodes is zero (—);  $\gamma_{LG}$ ,  $\gamma_{SG}$  and  $\gamma_{SL}$  are the surface tensions at the liquid/gas (air), solid/gas and solid/liquid interfaces, respectively, and  $V$  is the applied voltage.

liquid/gas interface  $\gamma_{LG}$ , the initial contact angle  $\theta_0$  and the applied potential  $V$  [Eq. (1)]:

$$\cos \theta = \cos \theta_0 + \frac{1}{2} \frac{1}{\gamma_{LG}} \frac{\epsilon_0 \epsilon}{d} V^2 \quad (1)$$

where  $\epsilon_0$  is the vacuum permittivity ( $8.854 \times 10^{-12} \text{ F m}^{-1}$ ),  $\epsilon$  is the dielectric constant of the dielectric material, which determines the ability of the dielectric layer to store charge, and  $d$  is the thickness of the dielectric layer. This equation allows us to predict the type of surfaces for which electrowetting may be effectively applied. It also describes how the degree of electrowetting can be controlled by moderating both the applied voltage ( $V$ ) and the properties of the optional underlying dielectric layer ( $\epsilon$  and  $d$ ).

Electrowetting has been successfully used in a number of studies to control the contact angle of liquid droplets.<sup>[10–39]</sup> Lippmann is believed to be the first to have recognised the effect of electrostatic charge on capillary forces at a liquid/liquid interface using mercury and an electrolyte in 1875<sup>[18,40]</sup> and to quantitatively formulate electrowetting shortly thereafter.<sup>[19]</sup> Other early examples of electrowetting include work by Froumkin<sup>[20]</sup> and Grahame,<sup>[21]</sup> who applied a potential to a solid/liquid (metal/electrolyte) and liquid/liquid (mercury/electrolyte) interface in the 1930s and 1940s. Minnema et al.<sup>[22]</sup> made a further advance in 1980 by adding a polymeric material between the hydrophobic layer and bottom electrode, which acts as a dielectric or insulating layer (Figure 1). This layer can store charge and enhance the electrowetting effect. Berge<sup>[23]</sup> carried out similar experiments with a dielectric layer, which effectively produced large changes in droplet contact angles. This phenomenon was named “electrowetting on insulator-coated electrodes” (EICE) by Quilliet and Berge,<sup>[18]</sup> while Moon and colleagues<sup>[13]</sup> coined the term “electrowetting on dielectric” (EWOD).

One desirable feature for operative electrowetting is a highly responsive surface, where small changes in voltage ( $V$ ) induce large changes in surface tension and droplet contact angle ( $\theta$ ). Equation (1) suggests that the voltage required for a certain contact-angle change can be decreased by using a material with a high dielectric constant or by reducing the thickness of the dielectric layer. Using this phenomenon, Saeki

et al.<sup>[11]</sup> and Moon et al.<sup>[13]</sup> performed EWOD experiments with thin dielectric layers and reduced applied voltages. Saeki et al. obtained irreversible electrowetting on a teflon-coated surface with an applied potential of only 6 V.<sup>[11]</sup> Saeki's strategy was to decrease the thickness of the dielectric layer, improve the dielectric film homogeneity and smoothness and to decrease the droplet volume. The addition of silicone oil to teflon surfaces was also used to improve the reversibility of the electrowetting effect, an observation supported by Lee et al.,<sup>[27]</sup> who reported that silicone oil minimises the effect of trapped charge and contact-angle hysteresis.

Increasing the thickness of the dielectric layer beyond 10  $\mu\text{m}$  can reduce charge accumulation at the liquid/surface interface, thus reducing electrowetting and necessitating high voltages.<sup>[10,15,24–26]</sup> Nevertheless, Welters et al.<sup>[24]</sup> demonstrated fast and reversible switching of 0.1 mm  $\text{KNO}_3$  water droplets on teflon surfaces between contact angles of 110 and 60° by applying voltages up to 200 V. Verheijen et al.<sup>[25]</sup> also demonstrated reversible electrowetting between 120 and 60° with voltages between –240 and 240 V using an aqueous droplet on a 30-nm teflon hydrophobic surface that was impregnated with silicone oil and featured a 10- $\mu\text{m}$  underlying parylene insulating layer. The charge remained in the liquid and was not trapped within or on the surface of the insulating layer at voltages between –240 and 240 V. At voltages greater than 240 V, however, the charge was trapped in the insulating layer, which led to a threshold-like behaviour. This phenomenon limits the induced charge density in the liquid droplet, thus preventing any further changes in contact angle.

Other recent publications<sup>[13,14,17,19,27–34,36,37]</sup> have used electrowetting for pumping liquids in microfluidic channels both with and without the optional dielectric layer. Moon et al.<sup>[13]</sup> presented a comprehensive study of pumping fluids in microchannels. They used dielectric materials with low and high dielectric coefficients [thin films of amorphous fluoropolymer (teflon AF) or silicon dioxide ( $\text{SiO}_2$ ) and barium strontium titanate (BST), respectively] and altered the thickness of the dielectric layer. Their study demonstrated that by increasing the dielectric constant and decreasing the thickness of the dielectric layer, the voltage required for reliable pumping of droplets could be lowered.

The majority of studies to date have used teflon as the hydrophobic layer or the dielectric layer, but electrowetting can be achieved on a variety of other polymer surfaces.<sup>[10,29]</sup> For example, Kuo et al.<sup>[29]</sup> achieved a 27° change in droplet contact angle by applying a voltage of 500 V to a polydimethylsiloxane (PDMS) film (Figure 2). In that study the electrowetting behaviour was highly similar for droplets of either deionised water or a solution of 100 mM KCl. These experiments demonstrate the versatility and broad potential of the electrowetting technique and pave the way for studies using more complicated aqueous solutions containing salts and buffers.

Vallet et al.<sup>[10]</sup> made a further observation of electrowetting on polymers that has implications for the reversibility of the electrowetting process. Their study on surfaces coated with poly(ethylene terephthalate) (PET) films found that the contact angle of water could be reduced by as much as 30° using high



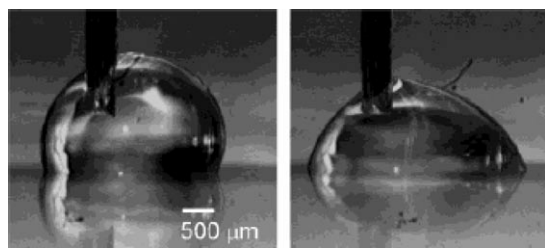


**Figure 2.** Surface wetting prior to (left) and after (right) the application of  $-500$  V to a PDMS-coated surface with a droplet of  $100$   $\mu\text{m}$  KCl solution. Reprinted with permission from ref. [29]. Copyright (2003) American Chemical Society.

voltages, but that this change was irreversible at all voltages above  $150$  V and that water droplets remained spread even when the voltage was decreased. This phenomenon was due to the permanent hydrophilic modification of the polymer film at the droplet edge. In contrast, the polymer surface under the liquid drop remained hydrophobic.

Superhydrophobic and superhydrophilic surfaces have the potential for even more pronounced surface switching. Superhydrophobic surfaces are exceptionally difficult to wet, and water droplets placed on these surfaces form a contact angle of at least  $150^\circ$ , while superhydrophilic surfaces are particularly easy to wet, and water will form a contact angle of approximately  $0^\circ$  with these surfaces. The properties and fabrication of these structures were well-documented in a recent review.<sup>[41]</sup> Superhydrophobic surfaces have been successfully fabricated by the alignment of carbon nanotubes and polymer nanofibres.<sup>[42,43]</sup> Superhydrophobic surfaces made from silicon nanowires and coated with fluoropolymer  $\text{C}_4\text{F}_8$  have also been rendered less hydrophobic, thus demonstrating a change in contact angle of  $23^\circ$  when  $150$  V was applied.<sup>[44]</sup>

A summary of the effect of electrowetting variables, including the dielectric material, dielectric constant, thickness of the dielectric layer and the applied voltage on the degree of surface wetting, measured by the contact-angle change, is presented in Table 1.

<b>Table 1.</b> Change in surface wetting and contact angle for aqueous droplets on a hydrophobic surface as a function of electrowetting variables including dielectric material, dielectric constant, thickness of the dielectric layer and applied voltage.					
Dielectric material	Relative dielectric constant [ $\text{F m}^{-1}$ ]	Thickness [ $\mu\text{m}$ ]	Actuation voltage [V]	Contact angle change [ $^\circ$ ]	Reference
silicon dioxide ( $\text{SiO}_2$ )	3.8	0.1 1	20–25 65–80	40	[13]
silicon nitride ( $\text{Si}_3\text{N}_4$ )	7.8	0.1	$\approx 23$	40	
polyethylene ( $\text{C}_2\text{H}_4$ ) <sub>n</sub>	2.95–3.15	12	$> 220$	40	
BST or ( $\text{Ba,Sr}$ ) $\text{TiO}_3$	$\approx 180$	0.07	$< 15$	40	
polytetrafluoroethylene- <i>ran</i> -[2,2-bis(trifluoromethyl)-4,5-difluoro-2H-1,3-dioxole]	1.93	0.013–1.6	5–55	15	
(teflon AF) ( $\text{C}_2\text{F}_4$ ) <sub>n</sub> ( $\text{C}_5\text{F}_8\text{O}_2$ ) <sub>m</sub>					
PDMS or ( $\text{H}_3\text{C}$ ) $[\text{SiO}(\text{CH}_3)_2]_n\text{Si}(\text{CH}_3)_3$	2.3–2.8	38	500	27	[29]
PET or ( $\text{C}_{10}\text{H}_8\text{O}_8$ ) <sub>n</sub>	3.65	12	200 <sup>[a]</sup>	30	[10]

[a] An effective actuation voltage was applied as an alternating current.

Another factor that may influence electrowetting and that remains largely unexplored is the configuration of the top electrode (Figure 1). This electrode is typically constructed from an inert material to avoid chemical interactions with the liquid droplet. We believe that both the electrode shape and the distance between the top and bottom electrodes will have a significant effect on the distribution of the electric field and degree of electrowetting. A further area that has not been fully investigated is the type of voltage stimulus used for electrowetting: positive and negative voltages may result in subtly different changes in contact angle.<sup>[13]</sup> The application of electrowetting has, to our knowledge, only been applied to make hydrophobic surfaces more hydrophilic and has not been used to increase surface hydrophobicity by neutralising existing charges present on a surface.

Electrowetting clearly shows great promise as a method for altering surface properties in a controlled manner. This potential is exemplified by recent optofluidic devices, which use electrowetting pumps to modulate the transmission characteristics of fibre structures<sup>[34]</sup> or the dynamic tuning of narrow- and broadband fibre filters.<sup>[14,33]</sup> Such devices can be applied to optical communications systems, and perhaps more widely, where they will have a significant impact on the functionality and control of material properties.

## Electrochemical Switching

The application of a voltage to a surface can change the chemical properties as well as the wettability. This process is referred to as electrochemical switching. One subset of electrochemical switching is an electrically induced change in redox state.<sup>[4,45–52]</sup> Surfactants with redox-active groups, for example, can be oxidised by an electric charge to generate cations. The presence of these cations then increases the wettability of the surface and reduces the contact angle of aqueous droplets in contact with the surface (Figure 3). When the potential is withdrawn, the active surfactant groups are reduced, thus restoring the surface hydrophobicity.

Various researchers<sup>[4,45–51]</sup> have reported successful electrochemical wetting using surfactants containing a redox-active ferrocene (Fc) group. Sondag-Huehthorst et al.<sup>[45]</sup> demonstrated that a voltage can be used to oxidise the Fc groups of Fc-terminated alkanethiols ( $\text{FcCO}_2\text{C}_{11}\text{H}_{22}\text{SH}$ ), which generates  $\text{Fc}^+$  cations that increase the surface wettability whilst still leaving the alkanethiol monolayer intact. They found that the contact angle can be switched reversibly between  $49$  and  $59^\circ$  for a mixed monolayer containing 60%  $\text{FcCO}_2\text{C}_{11}\text{H}_{22}\text{SH}$  and 40%  $\text{C}_{12}\text{H}_{25}\text{SH}$  (alkanethiol), and they

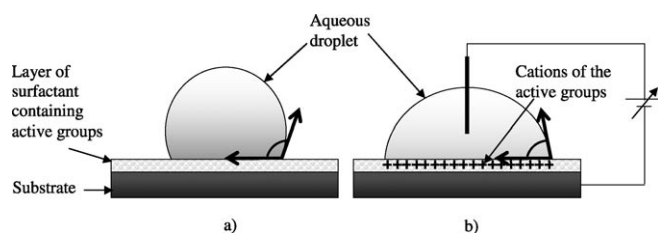


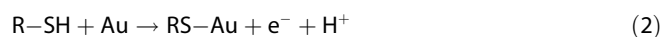
**Figure 3.** Schematic illustration of a cationic electrochemically switchable surface. a) When no voltage is applied the surface is hydrophobic; b) when voltage is applied the cations of the redox-active groups in the surfactant layer render the surface hydrophilic.

attributed these changes to specific interactions between the positively charged  $\text{Fc}^+$  ion and anions from the electrolyte.

Similar experiments by Abbott and Whitesides<sup>[4]</sup> showed potential-dependent wetting for aqueous droplets of 0.1 M  $\text{NaClO}_4$  on self-assembled monolayers (SAMs) constructed from 15-(ferrocenylcarbonyl)pentadecanethiol [ $\text{FcCO}(\text{CH}_2)_{15}\text{SH}$ ] on gold surfaces. They demonstrated a decrease in contact angle from  $71$  to  $43^\circ$  when the electrical potential was increased from  $0.3$  to  $0.5$  V. Gallardo et al. demonstrated analogous behaviour using  $\text{Fc}(\text{CH}_2)_{11}\text{N}^+(\text{CH}_3)_3\text{Br}^-$ .<sup>[46,49]</sup> Moreover, they were able to show pumping of droplets of the nematic liquid crystal 4-*n*-pentyl-4'-cyanobiphenyl through a simple fluidic network by applying potentials of  $+0.3$  and  $-0.3$  V, respectively, to oxidise and reduce  $\text{Fc}(\text{CH}_2)_{11}\text{N}^+(\text{CH}_3)_3\text{Br}^-$ .<sup>[46]</sup>

Another approach to electrochemical wetting, taken by Riskin et al.,<sup>[52]</sup> is to exploit the properties of a  $\text{Ag}^+$ -biphenyldithiol (BPDT) monolayer formed on a gold surface. They were able to control the hydrophobic properties of this surface by using an electrochemically induced transformation between the  $\text{Ag}^+$ -BPDT and  $\text{Ag}^0$ -BPDT states. When  $-0.2$  V is applied,  $\text{Ag}^+$ -BPDT is reduced to  $\text{Ag}^0$ -BPDT, and silver nanoclusters are generated on the surface. The resulting  $\text{Ag}^0$ -BPDT monolayer is more hydrophilic, and a droplet of  $0.1$  M  $\text{H}_2\text{SO}_4$  forms a contact angle of  $48$ – $52^\circ$  with the surface. When  $0.2$  V is applied, the monolayer is oxidised to  $\text{Ag}^+$ -BPDT, and the surface becomes less hydrophilic and returns to the original state with droplets forming a contact angle of  $\approx 64^\circ$ .

Thiol chemistry has also been used to develop innovative electrochemical switches that employ reductive electrochemical desorption.<sup>[5,53–58]</sup> SAMs are first constructed by reaction of a deprotonated thiol group with a surface. This reaction can be described for a gold surface by [Eq. (2)]:



where SH is the thiol group and R is the chain connected to thiol. The thiol bond formed between the monolayer and the gold surface is electrochemically reversible, and the application of a voltage negative to the desorption potential can then be used to desorb the monolayer from the gold surface to form thiolates ( $\text{RS}^-$ )<sup>[5]</sup> [Eq. (3)]:



Thus, application of a negative potential releases the hydrophobic SAM and restores the surface hydrophilicity (Figure 4). A further advance, reported by Porter and co-workers,<sup>[58]</sup> is

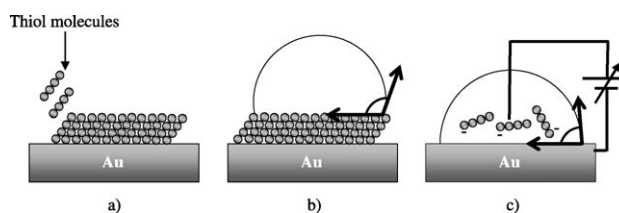


**Figure 4.** Schematic illustration of a thiol electrochemically switchable surface. a) Formation of a thiol-containing SAM on a gold surface (Au), b) hydrophobic thiol SAM surface prior to the application of a voltage, and c) hydrophilic Au surface following the application of a negative voltage, where the SAM is desorbed from the Au surface.

that the surface switching can be reversible. If an appropriate alkanethiol is selected, the SAM can be re-formed spontaneously when the electrical potential is lowered below the voltage required for desorption. In this way, the surface can alternate between hydrophilic and hydrophobic properties.

Utilising the thiol–gold linkage, Mali et al.<sup>[5]</sup> recently demonstrated the programmed electrochemical release of immobilised nanoparticles and biomolecules, including protein and DNA, from patterned gold electrodes. They successfully released fluorescently labelled avidin or 40-nm polystyrene (PS) nanoparticles from the uniformly coated electrodes after applying  $-1.5$  V to phosphate-buffered saline at pH 7.4, as illustrated in Figures 5a and 5b, respectively. The fluorescence intensity from adsorbed avidin decayed exponentially to near zero within 70 s (Figure 6), as protein was completely removed from the electrode. Protein release could also be tuned by reducing the applied voltage.

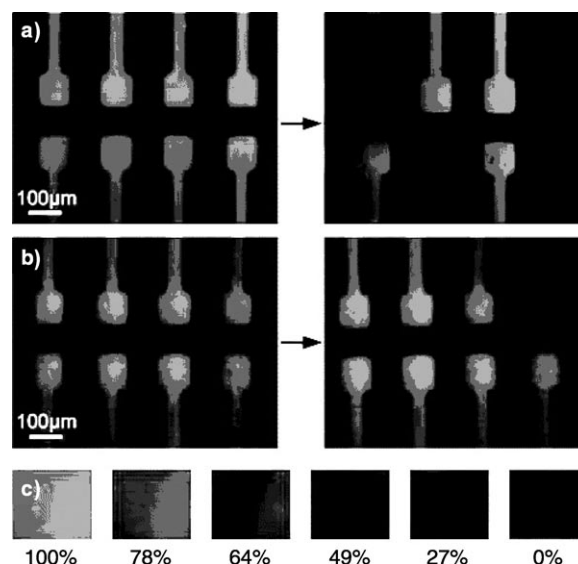


**Figure 5.** Fluorescence images showing electrochemically programmed release of a) fluorescently labelled avidin and b) fluorescently labelled 40-nm PS nanoparticles. This release is limited to selectively patterned gold micro-electrodes. c) Fluorescence intensity scale indicating electrode coverage for images in (a) and (b). Reprinted with permission from ref. [5]. Copyright (2006) American Chemical Society.

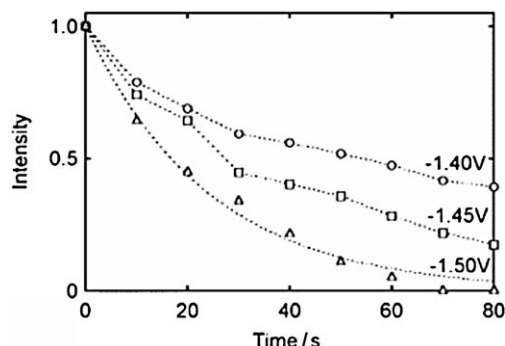


**Figure 6.** Release of fluorescently labelled avidin from modified gold electrodes with the application of  $-1.40$ ,  $-1.45$  and  $-1.50$  V. Reprinted with permission from ref. [5]. Copyright (2006) American Chemical Society.

Abbott et al.<sup>[53]</sup> successfully demonstrated similar switchable behaviour for a gold surface. The contact angles of aqueous solutions of electrolytes were found to be  $80$  and  $110^\circ$  at neutral potentials on SAMs of  $\text{CH}_3(\text{CH}_2)_{15}\text{SH}$  and  $\text{CH}_3(\text{CH}_2)_2\text{SH}$ , respectively, and became hydrophilic (contact angle of about  $10^\circ$ ) at less than  $-1.3$  V. According to Porter and co-workers,<sup>[58]</sup> different electrochemical potentials are required to desorb SAMs formed by alkanethiols of different chain length. They suggest that this phenomenon can be exploited to develop highly selective electrowetting, with shorter-chain SAMs desorbing at lower voltages than their longer counterparts. We envisage surfaces patterned with SAMs where sequential desorption occurs in different areas as the voltage is increased, or mixed SAMs where the monolayer density is reduced in discrete and sequential stages, thus allowing an advanced level of control over surface properties. Such surfaces would potentially be useful in drug delivery and related applications.

Electrochemically switchable surfaces can also be created using molecules such as 16-mercaptohexadecanoic acid (MHA). Low-density SAMs (LD-SAMs) of MHA on gold can undergo conformational transitions resulting in a change in surface properties.<sup>[55]</sup> MHA molecules consist of a hydrophobic chain capped with a hydrophilic carboxylate group. Derivatives of MHA which also contain an additional bulky globular head group can be used to space the MHA chains and to construct the LD-SAM.<sup>[55]</sup> Once the head group is removed, the spacing between MHA molecules allows the chains to undergo the conformational transition required for surface switching.

Upon application of electrical potential, the negatively charged carboxylate groups experience an attractive force to the gold surface, and the chains bend towards the surface, thus exposing the hydrophobic section of the MHA molecule to the solution (Figure 7). Lahann et al.<sup>[55]</sup> demonstrated that this principle can successfully be applied to reversibly switch the surface hydrophobicity.

Mu et al.<sup>[54]</sup> used a similar approach but applied cyclodextrin molecules as space fillers between the MHA molecules for the construction of LD-SAMs. The cyclodextrin groups could be removed by treatment with solvents, thus leaving an effective surface for electrochemical switching. Mu and colleagues used applied potentials to alter the conformation of the MHA

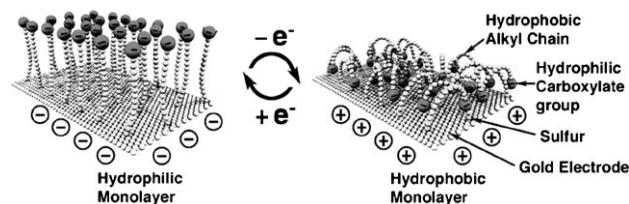


**Figure 7.** Schematic representation of the transition between hydrophilic (straight) and hydrophobic (bent) molecular conformations for MHA molecules upon application of voltage. MHA molecules assemble via thiol interactions with the surface and are capped with a hydrophilic carboxylate group. Reprinted with permission from ref. [55]. Copyright (2003) Science.

groups and selectively assemble charged proteins, such as avidin and streptavidin, on the surface.

Electrochemical switching can be applied to control surface passivation and biomolecule interactions. Tang et al.<sup>[56]</sup> passivated an indium tin oxide (ITO) microelectrode array by uniformly coating the surface with a protein-resistant poly(L-lysine)-*graft*-polyethylene glycol (PLL-*g*-PEG) copolymer. The application of a  $+1.8$ -V electric potential to individual ITO microelectrodes resulted in the localised release of the polymer, which revealed a bare ITO surface for subsequent biological immobilisation. Different biological molecules and nanoparticles were adsorbed onto the activated ITO microelectrodes while other regions remained protein-resistant. These adsorbed biomolecules retained their functionality. For example, streptavidin was able to bind biotinylated vesicles. Desorption of the PLL-*g*-PEG was found to be highly selective, rapid and reversible, thus indicating that this approach could be widely applied to control molecular interactions.

Electrochemical control can also moderate the interaction of DNA molecules with a surface. Hook et al.<sup>[57]</sup> demonstrated electrostimulated adsorption and desorption of DNA by surface modification of highly doped p-type silicon. They deposited an amine-rich allylamine plasma polymer and then grafted high-density poly(ethylene oxide) on the surface. These layers support and resist DNA adsorption, respectively. High-resolution patterns of re-exposed plasma polymer were then produced using an excimer laser, which created regions for spatially controlled adsorption of DNA. In a specially designed flow cell, they applied positive ( $0$  to  $+2$  V) and negative ( $0$  to  $-2$  V) voltages to the surface with a platinum-wire counter electrode for approximately  $2$  min to demonstrate DNA adsorption and desorption. This study was directed towards increasing the efficiency of DNA transfection of cells, but this technology could be applied to great effect for the delivery of DNA, RNA or oligonucleotides for other purposes, such as microfluidic channels for polymerase chain reactions where nucleic acid signals can be amplified for easy detection.

In general, electrochemical switching involves the application of smaller voltages than electrowetting. This makes the technique particularly suitable for biological applications in which the use of smaller voltages is desired. Consequently, research to date has focused on electrochemical surface patterning and release of biomolecules from surfaces. Two notable applications include the patterning of microfluidic devices with

multiple types of antibodies<sup>[6]</sup> and the patterning of cell surfaces to manipulate and constrain cell movement across a surface.<sup>[59]</sup>

In some situations the electrochemical release of molecules can serve a function, while in other cases it introduces an undesirable waste product into the immediate environment surrounding the surface. An additional challenge in this area is to fully understand the process of electrochemical switching including changes at a small scale, such as the presence of surface charges or ions, and the possible effect of a dielectric double layer. Greater understanding of the fundamental process will also allow the full control of molecular patterning and release, and ensure that biomolecules have optimal orientations and functionality.

## Photoswitching

Photoinducible surfaces respond to electromagnetic radiation and result in photoswitching. Artificial photostimuli or light fluctuations in the natural environment can be used to trigger reversible geometric isomerism of molecules from a *cis* to a *trans* conformation, reversible dimerisation or reversible ring opening, which result in changes to the surface hydrophobicity.

Azobenzene units are particularly promising photoresponsive structures and many studies<sup>[3,47,60–63]</sup> have demonstrated the reversible isomerisation of azobenzene rings incorporated into surface coatings, which leads to an increase in surface wettability. This process is illustrated in Figure 8. Ichimura

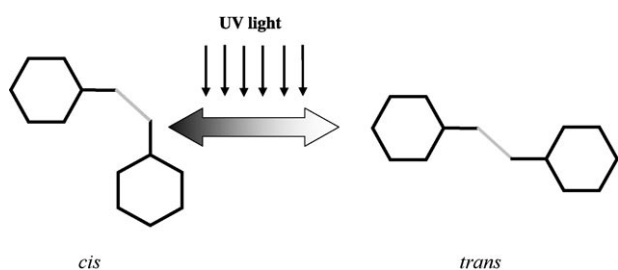


**Figure 8.** Geometric isomerism of azobenzene units from a *cis* to a *trans* conformation by illumination with UV light. The *cis* conformation of the azobenzene unit is more hydrophobic than the *trans* conformation.

et al.<sup>[60]</sup> demonstrated a change in surface energy following photoirradiation of a liquid droplet on a substrate modified with a calix-resorcinarene derivative containing azobenzene units. They were able to tune the direction and velocity of the motion for the target liquid by varying the direction and gradient in light intensity. Azobenzene side chains also featured in monolayers on silicon, which experienced a decrease in contact angle of 9° when irradiated with light at 354 nm,<sup>[64]</sup> and in monomolecular films of poly(vinyl alcohol)s (PVAs),<sup>[65–68]</sup> in which the azobenzene units were responsible for the large reversible expansion and retraction of the film in response to UV and visible light.

A different approach was pursued by Sakai et al.<sup>[69]</sup> who used the isomerisation of azobenzene units to control vesicle formation and stability in aqueous suspensions. Their system included an azobenzene-modified cationic surfactant [4-butylazobenzene-4'-(oxyethyl)trimethylammonium bromide] mixed with an anionic surfactant (sodium dodecyl benzenesulfonate). Similar photoisomerisation results are reported by Shin and Abbott<sup>[3]</sup> using a mixed surfactant system containing sodium dodecyl sulfate and 4,4'-bis(trimethylammoniumhexyloxy)azobenzene bromide, and the authors suggest that such vesicles have potential applications as vessels for the delivery of drugs or perfumes, as solubilising agents for removing hydrophobic compounds from waste water<sup>[69]</sup> or as agents to assist coating and liquid spreading on microanalytical devices.<sup>[3]</sup>

Photoinduced dimerisation has been employed by Abbott et al.<sup>[70]</sup> to decrease the wettability of a pyrimidine-terminated monolayer assembled on gold or quartz substrates. The structure of pyrimidine is wavelength-dependent. Abbott and colleagues irradiated the surface with UV light with a wavelength of 280 nm to induce dimerisation and increase surface hydrophobicity or 240 nm to cleave the dimer and restore the surface properties. They found that SAMs constructed from long-chain thymine-terminated thiols gave the largest, reversible photoinduced change in contact angle of 26°. In contrast, uracil SAMs showed an irreversible change in contact angle of 16°, and irradiation with light at 240 nm did not restore the monomer or surface hydrophobicity. Photoinduced dimerisation has also been demonstrated by Wolf and Fox for a *cis*-4-cyano-4'-(10-thiodecoxy)stilbene monolayer on a gold surface treated with visible light at >350 nm, and surface patterns could be created using this technique.<sup>[71]</sup>

Photoactivated control of ring structures has been shown by Bunker et al.,<sup>[72]</sup> who demonstrated that UV and visible light can be used to open and close a significant fraction (10–20%) of ring structures in spiropyran films. In aqueous solutions and other proton-donating solvents, ring opening results in a positively charged surface that increases the surface hydrophilicity. The ring structure in spiropyran films can also undergo reversible isomerisation from a relatively nonpolar structure to a polar isomer by exposure to UV or visible light. Rosario et al.<sup>[73]</sup> demonstrated a decrease in contact angle of 11–14° when dry spiropyran-coated surfaces were treated with UV irradiation.

Superhydrophobic surfaces can also be responsive to photostimuli. Feng et al.<sup>[7]</sup> were the first to report a reversible superhydrophobicity to superhydrophilicity transition on aligned ZnO nanorod films (Figure 9) by alternating UV illumination

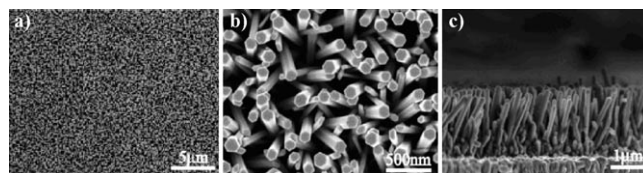


**Figure 9.** a) and b) Scanning electron microscopy images of the upper surface of ZnO nanorod films at low and high magnifications, respectively. c) Cross-sectional view of the vertically aligned ZnO nanorods. Reprinted with permission from ref. [7]. Copyright (2004) American Chemical Society.



with dark storage. The surface features that are thought to contribute to the properties of superhydrophilic surfaces include electron–hole pairs generated during UV irradiation.<sup>[74]</sup> These electrons can react with lattice oxygen to form surface oxygen vacancies. Water and oxygen may compete to adsorb at these sites, but the adsorption of hydroxyl groups is more kinetically favoured than the adsorption of oxygen. In the short term this results in hydroxyl adsorption and improved surface hydrophilicity. For a rough surface, water also enters and fills the grooves of the films, thus leaving only the top part of the nanorods exposed from the liquid. This behaviour is similar to the three-dimensional capillary effect of a rough surface.<sup>[75,76]</sup>

The superhydrophilic effect on a UV irradiated surface is only temporary, and the surface becomes energetically unstable following the adsorption of hydroxyl groups. These groups are gradually replaced by oxygen atoms, which bond more strongly to the defect site. When the UV-irradiated films are placed in the dark, the surface evolves back to its original state (before UV irradiation), and the wettability is reconverted from superhydrophilic to superhydrophobic.<sup>[74]</sup> Similar results are also found for TiO<sub>2</sub> surfaces.<sup>[77]</sup> Feng et al.<sup>[7]</sup> used this technique to demonstrate complete wetting (a change in contact angle from 162 to 0°) on ZnO films by UV illumination for 2 h (Figure 10).

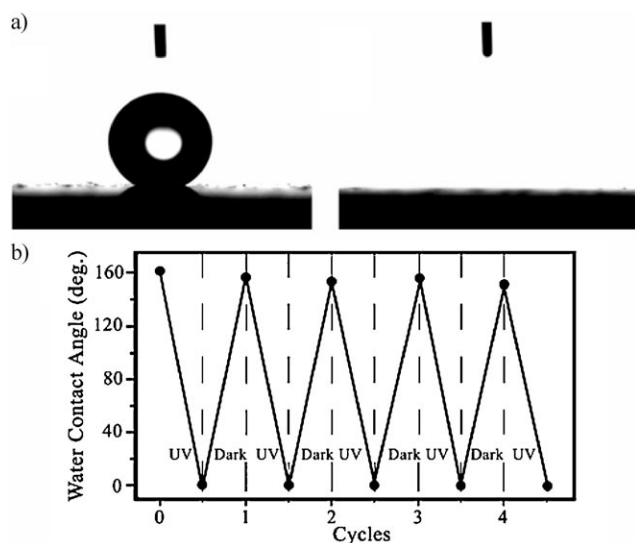


**Figure 10.** a) Images of water-droplet shape on aligned ZnO nanorod films before (left) and after (right) UV illumination. b) Reversible superhydrophobic and superhydrophilic transition of ZnO films exposed to alternating UV irradiation and dark storage. Reprinted with permission from ref. [7]. Copyright (2004) American Chemical Society.

As a drawback, Hiroshi et al.<sup>[78]</sup> reported that ZnO suffers from photocorrosion and is unstable under UV light compared to other UV-stable metal oxides, such as TiO<sub>2</sub>, which is a well-known photocatalyst. They demonstrated a contact-angle switch between 130 and 0° before and after UV illumination, respectively, on a fluoroalkylsilane-treated TiO<sub>2</sub> surface.

One of the distinct advantages of photoinduced thermal switching is that the stimulus does not induce electrical or mechanical noise. A disadvantage, however, is that UV light is hazardous and can cause permanent damage to biomolecules such as DNA. Light present in the environment can be used to trigger surface changes but could also be problematic, and the light intensity required in each case is not always documented. The long- and short-term stability will also be critical to the application of these surfaces. Photoswitching does, however, produce substantial changes in contact angle, unlike the two previous electroactivation methods.

## Thermal Switching

The thermal switchability of surfaces is primarily based on utilisation of the lower critical solution temperature (LCST) of polymers, above which a polymer becomes insoluble in water and below which swelling occurs that makes the surface hydrophilic. One polymer that has been successfully employed as a thermally responsive film is poly(*N*-isopropylacrylamide) (PNIPAAm). Several researchers report that these films can be switched between hydrophilic and hydrophobic states in response to relatively small changes in temperature.<sup>[79–84]</sup> Such thermally switchable surfaces can be applied not only in the built environment but also in the natural environment, where natural temperature fluctuations could be used to alter material properties and functionality.

Sun et al.<sup>[79]</sup> proposed a mechanism for the thermal switching of PNIPAAm films, which is outlined in Figure 11. They suggest that intermolecular hydrogen bonding between the PNIPAAm chains and water molecules is a major contributor towards PNIPAAm film hydrophilicity at temperatures below the

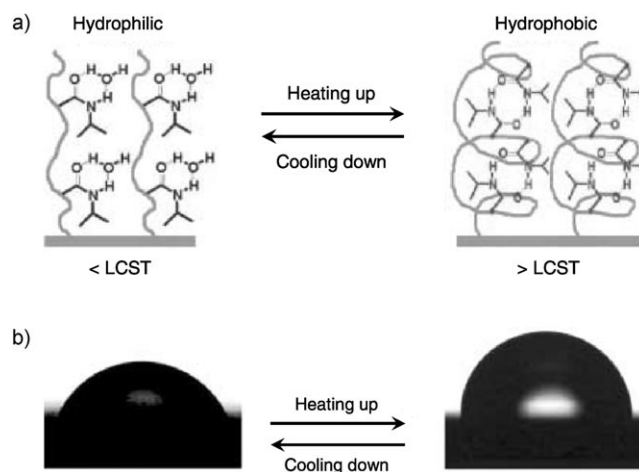


**Figure 11.** Thermally responsive wettability for a PNIPAAm-modified surface. a) Diagram illustrating the switch between a hydrophilic and hydrophobic surface. PNIPAAm chains are shown forming intermolecular hydrogen bonds with water molecules at temperatures below the LCST (left) and forming intramolecular hydrogen bonds between C=O and N–H groups at temperatures above the LCST (right). This bonding is considered to be the molecular mechanism of the thermal response and change in wettability. b) The change in surface wettability when the temperature is raised from 25 °C (left) to 40 °C (right), which induces a change in the water contact angle from ≈ 64 to ≈ 93°. Reprinted with permission from ref. [80].

LCST (Figure 11 a). At temperatures above the LCST, intramolecular hydrogen bonding between C=O and N–H groups in the PNIPAAm chains is thought to result in the chains adopting a collapsed conformation, which makes it difficult for the hydrophilic C=O and N–H groups to interact with water molecules (Figure 11 a). Thus, the film is hydrophobic at high temperatures. Sun and colleagues applied this theory, and demonstrated a change in water contact angle of approximately 30° for water droplets on PNIPAAm-modified surfaces by increasing the temperature from 25 to 40 °C (Figure 11 b).

Huber et al.<sup>[80]</sup> utilised thermal switching to develop a microfluidic device with the capacity to adsorb large globular proteins from solution and subsequently release these proteins on command. Their study employed a 4-nm-thick PNIPAAm layer which exhibits an LCST of approximately 35 °C in water. Below this temperature the film swells and interacts with water to create a relatively hydrophilic surface, with a water contact angle as low as 30°. Above the transition temperature, the polymer collapses as water is expelled and the surface becomes substantially less hydrophilic, with a water contact angle approaching 90°. The hydrophilic layer is passive and the hydrophobic surface can adsorb large proteins, such as haemoglobin and bovine serum albumin. Another important feature of this system is the response time for heating and cooling, which is < 1 ms and < 1 s, respectively.

Temperature-responsive surfaces can respond to additional triggers. Elastin-like polypeptides (ELPs), which contain repeats of a pentameric peptide sequence, not only undergo a switchable and reversible change in hydrophilicity in response to temperature but also change in response to changes in ionic strength or pH under isothermal conditions. For example, ELPs have been shown to undergo thermally induced aggregation when free in solution, and this phenomenon has been used as a low-cost method to purify fusion proteins containing an ELP tag.<sup>[8,85]</sup> ELP fusion proteins can also be captured on ELP-patterned surfaces by changes in ionic concentration.<sup>[86]</sup>

Hyun et al.<sup>[87]</sup> have exploited changes in ionic strength to induce phase transition behaviour for ELP-functionalised surfaces. They reversibly immobilised thioredoxin–ELP (Trx–ELP) fusion proteins on ELP nanostructures that had been grafted onto  $\omega$ -substituted thiolates. These proteins were sterically accessible and could bind a Trx-specific antibody. Moreover, they could be released by further changes in ionic concentration.

Recently, Ebara et al.<sup>[88]</sup> developed a chromatographic device containing PDMS channels. They were able to reversibly adsorb and desorb stimuli-responsive bioanalytical beads, which could be used for fractionating, purifying and concentrating target analytes or more widely applied in immunoassays and enzyme bioprocesses.<sup>[88]</sup> Ebara and colleagues grafted PNIPAAm onto PDMS surfaces using UV light. Below the LCST, grafted surfaces demonstrated minimal contact angles of 35° and did not bind beads. Above the LCST, these surfaces demonstrated maximal contact angles of 82° and adsorbed beads. These materials are highly attractive as the contact angles may be tuned by selecting an appropriate graft density.

One challenge in the development of thermally induced switchable surfaces is to ensure that the change in tempera-

ture required to induce switching does not damage any solutions or biomolecules in close proximity to the surface. Many proteins, for example, are particularly sensitive to temperature change. The examples reviewed here, however, suggest that thermal switching may be successfully tailored to a wide range of applications including bioanalytical devices, proteomic functions,<sup>[80]</sup> chromatography,<sup>[88]</sup> controlled drug release and thermally responsive filters.<sup>[79]</sup>

Furthermore, thermally induced switchable surfaces are suitable substrates for the culture of a wide range of cell types.<sup>[89–92]</sup> These surfaces can be used for the gentle recovery of cell sheets containing single or multiple types of cells at low temperatures,<sup>[90]</sup> so that the majority of extracellular matrix components are retained within the cell monolayer.<sup>[91]</sup> The resulting cell sheets can then be manipulated and used for surgical applications.<sup>[92]</sup>

## Mechanical Switching

Mechanically switchable surfaces are based on the extension and relaxation of elastic surfaces. When an elastic film is extended the fibres or polymer chains within the film stretch, which makes the film hydrophilic (Figure 12). When the film is

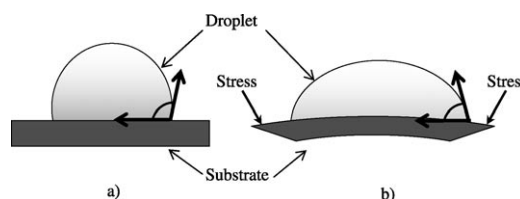


**Figure 12.** Mechanically responsive wettability. a) A surface is hydrophobic when no tension is applied. b) The same surface becomes hydrophilic when stress is applied, which stretches the film.

relaxed to the original state the fibres or chains shrink, thus restoring the film hydrophobicity.

Zhang et al.<sup>[93]</sup> reported a particularly interesting case of reversible mechanical switching between superhydrophobic and superhydrophilic surfaces, in which the bulk surface structure undergoes a dramatic change. They biaxially extended and unloaded an elastic polyamide  $[-(\text{CH}_2)_{11}-\text{CO}-\text{NH}-]_n$  film with a microscale triangular netlike structure (Figure 13). Each unit structure within the film consisted of a triangle with an average side length of approximately 200  $\mu\text{m}$  and an average fibre diameter of 20  $\mu\text{m}$  (Figure 13 a). The contact angle of water with this polyamide film was 151° (Figure 14). When the film was biaxially extended, to stretch the film by greater than 120% and extend each triangular structure to nearly 450  $\mu\text{m}$  in length (Figure 13 b), the water droplet spread into the space among the fibres and the contact angle of the droplet approached 0° (Figure 14). The mechanically induced hydrophilicity was only effective when at least 27  $\mu\text{L}$  of water contacted each unit area ( $\text{cm}^2$ ) of surface. If less water was present, the droplets could not flow down through the polymer web, and the film recovered its original state.

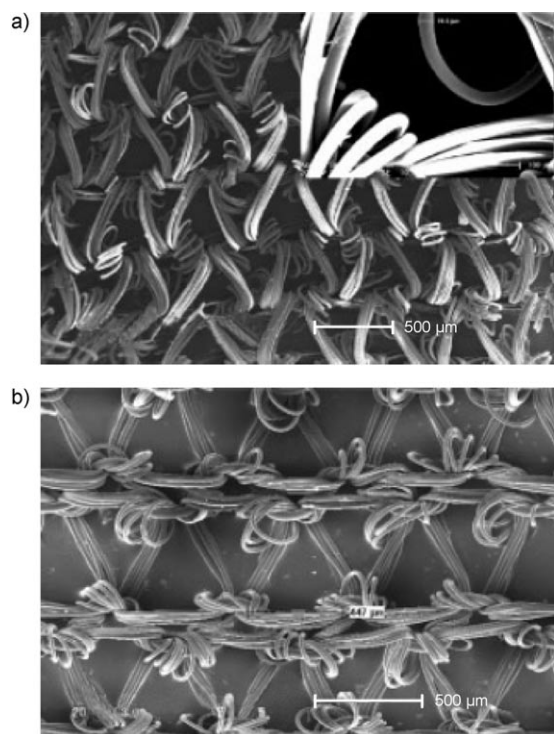


**Figure 13.** Scanning electron micrographs of polyamide films which show the triangular netlike structural units. a) Before biaxial extension the average side length of the triangular features is approximately 200  $\mu\text{m}$  and the fibre diameter is approximately 20  $\mu\text{m}$ . b) Following biaxial extension of the film by nearly 120%, the average side length of the triangle is extended to 450  $\mu\text{m}$ . Reprinted with permission from ref. [94].

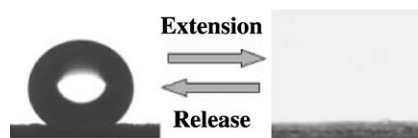


**Figure 14.** Mechanically induced switching between superhydrophobic and superhydrophilic surface properties for an elastic polyamide film with a triangular netlike structure (shown in Figure 13). Before biaxial extension or after release of the extensional load, the water contact angle is approximately 151° (left). Following extension of the film by 120% the water contact angle is reduced to 0° (right). Reprinted with permission from ref. [94].

A complementary approach was taken by Genzer et al.,<sup>[94]</sup> who reported that elastomeric surfaces can be tailored using mechanically assembled monolayers (MAMs). They developed a switchable surface by attaching perfluoroalkanes at specific graft points on a pre-stretched PDMS film. The perfluoroalkanes are hydrophobic with a water contact angle of approximately 100°. When the strain is released the elastomer relaxes, the density of the grafted molecules increases and the water contact angle increases by 30°, thus making the surface superhydrophobic.

These two examples of mechanically inducible surfaces both employ materials with uniform stress–strain properties. Future studies could seek to develop materials with nonuniform

stress–strain properties that display hydrophobicity gradients. Studies may also explore the effect of compressional loads on surface hydrophobicity. These surfaces could find applications as switches that respond to a stimulus, such as simple finger pressure.

## Environmental Switching

Surfaces that respond to changes in their immediate environment may be described as being environmentally responsive. Amphiphilic polymers belong to this class of surfaces. These polymers contain both hydrophilic and hydrophobic grafted groups or segments, as shown in Figure 15. They restructure in

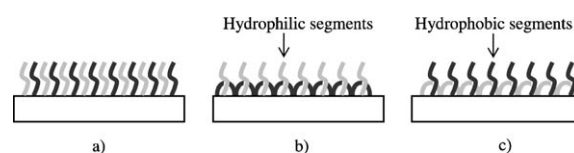


**Figure 15.** a) An environmentally responsive amphiphilic copolymer with hydrophilic (grey) and hydrophobic (black) segments. b) Restructuring of the polymer surface and enrichment of hydrophilic groups following exposure to a polar solvent. c) Restructuring of the polymer surface and enrichment of hydrophobic groups after treatment with nonpolar solvent or drying.

response to the polarity of a solvent: hydrophilic groups become enriched in a polar solvent and hydrophobic groups become enriched in response to a nonpolar solvent to minimise the surface energy (Figure 15b,c). Such solvents are said to be selective for one polymer component. Surface hydrophobicity can also be induced by drying the surface (Figure 15c). Numerous reports<sup>[95–121]</sup> have documented amphiphilic surfaces and their properties, including the selective adsorption and desorption of biomolecules. These surfaces hold great potential for applications such as chromatography and the development of smart biomaterials.

Mori et al.<sup>[96]</sup> reported the switchability of amphiphilic block copolymers containing PS, poly(4-octylstyrene) or polyisoprene as a hydrophobic segment and poly(2,3-dihydroxypropyl methacrylate) [poly(DIMA)] as a hydrophilic segment. Their copolymers were hydrophobic in air due to the enriched number of hydrophobic segments on the surface, but when soaked in water, hydrophilic groups were enriched on the surface. The hydrophobic surface could also be reconstructed by drying the sample in air.

Many research groups<sup>[97–106]</sup> have demonstrated similar reversible surface switching by employing amphiphilic polymers. Chen et al.<sup>[99]</sup> reported a switchable copolymer with poly(vinyl sugars) as hydrophilic pendant groups on PS, in which the contact angle could be decreased by 20–40° when surfaces were soaked in water. Senshu et al.<sup>[100–102]</sup> also demonstrated polymer rearrangement and replacement of hydrophobic groups at the uppermost surface with hydrophilic groups when soaking diblock and triblock copolymer films in water. Again, drying could be used to restore the hydrophobic surface.

On a similar theme, Vaidya and Chaudhury synthesised environmentally responsive polyurethanes containing PEG, PDMS and perfluoroether segments.<sup>[107]</sup> The resulting polymer becomes hydrophilic when exposed to water. The authors attribute this response to the reorientation of the PEG groups at the polymer/liquid interface. They also show that the polymer becomes hydrophilic when exposed to water vapour. This high sensitivity to a small volume of water is significantly different to some mechanically inducible surfaces outlined in the section above, where a large volume of water is required to achieve hydrophilicity. Moreover, this surface switching can be effectively tuned by varying the composition of the polymer segments, and such surfaces may be applied to resist dirt or bio-molecule fouling.<sup>[107]</sup>

Hester et al.<sup>[108]</sup> demonstrated reversible switching using an amphiphilic comb polymer constructed from a poly(methyl methacrylate) (PMMA) backbone with poly(ethylene oxide) side chains and blended with poly(vinylidene fluoride). This surface could be rendered hydrophilic or hydrophobic by annealing at elevated temperatures in the presence of water or acid, respectively. Hester and colleagues also found that higher fractions of the hydrophilic comb polymer imparted significant resistance to the adsorption of bovine serum albumin, which suggests a nonfouling surface.

Triblock polymers were used by Ishizone et al.<sup>[109]</sup> to achieve similar environmentally responsive surfaces. Polymers containing 2-(perfluorobutyl)ethyl methacrylate, *tert*-butyl methacrylate and 2-(trimethylsilyloxy)ethyl methacrylate formed micelles in selective solvents. Their study confirmed the enrichment of the 2-(perfluorobutyl)ethyl methacrylate segment at the surface of dry polymer films and the induced surface rearrangement in response to changes in environmental conditions.

Other research groups<sup>[110,111]</sup> have also investigated the use of binary polymer brushes to control wettability and produce surfaces with the capacity for high, medium and low surface hydrophilicity. For example, Uhlmann et al.<sup>[110]</sup> demonstrated surface switching of a binary polymer brush made from a hydrophilic polymer [poly(2-vinylpyridine)] and a hydrophobic polymer (PS). They observed hydrophilicity when surfaces were treated with polar solvents, hydrophobicity when surfaces were treated with a nonpolar solvent and intermediate contact angles when surfaces were treated with a solvent favoured by neither polymer component. They propose that polymer chains are in a stretched conformation in favourable solvents. In a nonfavourable solvent the chains experience repulsion, which leads to chain collapse and the formation of a coiled polymer conformation. In a solvent favoured by neither polymer component, the chains form laterally segregated lamella-like structures.

Two parallel studies by Lu et al.<sup>[112]</sup> and Zhao et al.<sup>[113]</sup> developed reversibly switchable surfaces from polystyrene-*block*-poly(methyl methacrylate) (PS-*b*-PMMA), which respond to block-selective solvents. Lu et al.<sup>[112]</sup> demonstrated a change of the water contact angle from 22.6 to 42.6° when films were treated with solvents selective for the PS or PMMA units, respectively. This behaviour is illustrated in Figure 16.

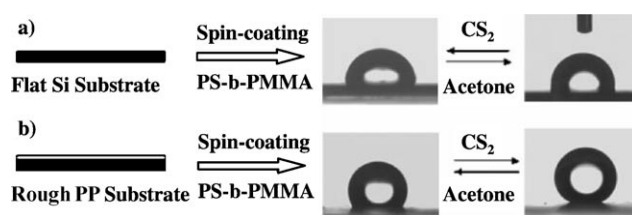


**Figure 16.** Schematic illustration of the fabrication of an environmentally responsive and reversibly switchable composite film. A thin film of PS-*b*-PMMA is deposited on a) flat silicon (Si), and b) rough isotactic poly(propylene) surface. The surfaces switch between hydrophilic and hydrophobic when treated with carbon disulfide (CS<sub>2</sub>) and acetone. Reprinted with permission from ref. [112].

Recently, Wang et al.<sup>[95]</sup> reported a switchable thin-film surface that was prepared by grafting a polystyrene-*block*-poly(2-vinylpyridine) (PS-*b*-P2VP) copolymer. They observed changes in the surface properties upon treatment with block-selective solvents; the advancing contact angles measured after tetrahydrofuran, isopropyl alcohol and cyclohexane treatment were 80, 75 and 80°, respectively. To further reduce the miscibility of the two polymer arms, they treated the film with methyl iodide to form quaternary ammonium groups on the P2VP block. After quaternisation, they measured the advancing contact angles to be 52 and 75° with water and cyclohexane treatment, respectively, which indicates that quaternisation was successful.

Another way of generating switchable polymeric surfaces is to graft Y-shaped binary molecules with two polymer arms to a surface.<sup>[114–120]</sup> These polymer arms can be two incompatible polymers, such as hydrophobic PS and hydrophilic poly(acrylic acid) (PAA). Selective solvents can then be used to induce conformational rearrangements in a controlled and reversible fashion. For example, Julthongpiput et al.<sup>[118]</sup> treated PS-PAA with toluene and water and demonstrated a change in water contact angle of 73 and 53°, respectively.

Lei et al.<sup>[119]</sup> were able to immobilise the enzyme pectinase onto PS-*b*-PAA microspheres in solution, which suggests that other enzymes may also be immobilised on surfaces grafted with PS-*b*-PAA. Amphiphilic polymers consisting of hydrophilic PAA and hydrophobic poly(butyl acrylate) have also been used to create polymer networks that swell in response to the pH value.<sup>[122]</sup> The successful release of drugs from these hydrogels suggests that this approach can be used to develop grafted polymer surfaces for controlled drug delivery.

Environmentally switchable surfaces are particularly smart materials that can be tuned or manipulated for specific applications. In addition, they offer the opportunity to modify surface texture in a controllable manner. One of the challenges in this area is the synthesis and deposition of the polymer film. Each new application will require a specific polymer type. Environmentally switchable surfaces are also often designed to be responsive to particular solvent types, which may not be compatible with aqueous chemistry but remain a cost-effective solution for industrial applications.



## Other Switching Methods

Other techniques exist to develop switchable surfaces with tailored hydrophobicity. These methods share similarities with the categories of switchable surfaces discussed so far, but are not easily classified within these categories

It is possible to utilise chemical reactions to tailor the switchability of surfaces.<sup>[123]</sup> Thanawala and Chaudhury<sup>[123]</sup> modified a PDMS elastomer using a hydrosilation reaction, in which an allyl amide functionalised perfluorinated ether (PFE) was incorporated into a siloxane network. They showed that the PFE migrates to the surface of the modified polymer, thus reducing the surface energy from 22 to  $\approx 8 \text{ mJ m}^{-2}$ . This decrease in surface energy results in an increase in dynamic advancing contact angle for water from 120 to 140°.

Hyperbranched polymers (HBPs) offer another avenue for developing responsive surfaces.<sup>[124–126]</sup> HBPs can be used as processing aids for linear low-density polyethylene (LLDPE), and Hong et al.<sup>[124]</sup> report that HBPs have a tendency to migrate to the surface of the polymer film to form a lubricating layer. This phase separation can be utilised to tailor unique surface properties. For example, Sendjarevic et al.<sup>[125]</sup> varied the length of alkyl terminal groups on polyetherimide (PEI) HBPs, which changed the polymer miscibility and altered the surface properties of PEI–HBP–LLDPE blends. Alkane substitution at the end of hydroxyl-terminated HBPs can also be used to reduce the surface tension generated by HBP layers.<sup>[126]</sup>

Mechanically interlocked molecules are of further interest for the development of smart molecular machines. Many research groups<sup>[127–136]</sup> have demonstrated surface switching using mechanically interlocked molecules, such as rotaxanes<sup>[137–141]</sup> and catenanes.<sup>[137,142–145]</sup> Rotaxanes are dumbbell-shaped molecules surrounded by a macrocyclic compound or ring. These rings are kept in place by two terminal bulky groups. Catenanes consist of two macrocyclic compounds or interlinked rings.<sup>[137]</sup> The noncovalent interactions between these components can be used to induce movement.

In the case of rotaxanes, the ring component of the molecule can be induced to move along the length of the dumbbell-shaped component by a change in proton concentration or by electrochemical<sup>[133,136]</sup> or photochemical means,<sup>[134,135]</sup> thus providing a versatile molecular machine. Importantly, such conformational changes can be induced when rotaxanes are bound to a surface either directly or through monolayers, and the reader is directed to an excellent overview of their potential use as artificial molecular muscles, enzymes, shuttles and lifts.<sup>[137]</sup>

A recent direction in the research and development of switchable surfaces is the combination of multiple trigger types to stimulate changes in surface wettability. These studies typically combine changes in pH and temperature to modify surface properties.<sup>[146–149]</sup> This approach may be applied to chromatography, microfluidic networks and biosensors, where it will offer an advanced level of control.

There are still many unexplored possibilities for designing custom switchable materials. For example, Russell<sup>[150]</sup> proposed that the thickness, composition and morphology within a film

can be gradually changed across a material in one or several directions to manipulate switchability. Nanoparticles may also be employed in the design of responsive materials. Particles may be surface functionalised with ligands and then tethered to the base of nanopores found within thin copolymer films. The embedded nanoparticles can then be stimulated to move up or down within the pores, thus exposing or hiding the interacting sites, in response to local environmental changes such as pH or temperature. With the development of novel nanostructured thin films, it is probable that the surface morphology of nanoscale structures will also play a major role in devices with intelligent surfaces.

## Conclusions and Future Directions

A large variety of external stimuli can trigger changes in surface hydrophobicity and wettability. We have discussed and categorised current research according to the types of stimuli, which include electrical, electrochemical, photonic, thermal, mechanical and environmental effects.

Several characteristics are likely to influence the development of intelligent surfaces and devices incorporating these surfaces. These properties, which are unique for each individual surface, include:

- The magnitude of the stimulus and the resulting change in surface wettability.
- The kinetics of any changes in surface wettability.
- The reversibility of surface switching.
- The tunability of the surface switching.
- The short- and long-term stabilities of the surface.
- The uniformity of the surface for the adsorption of chemical or biochemical components.
- The specificity of molecule adsorption on the surface or nonfouling properties.
- The conformation of molecules adsorbed on the surface and the resulting effect on surface wettability.
- The ease of molecule release from the surface.
- The changes in surface structure and texture resulting from switching or compound release.
- The ease and cost of surface fabrication.
- The ease and cost of surface switching.

The studies reviewed illustrate how researchers are already examining and addressing these factors. When combined with new ideas, the existing techniques promise to stimulate the development of a wide range of devices including smart molecular machines. One of the most promising applications for these devices will be as delivery agents for the release of biomolecules or biopolymers including small drugs, DNA, RNA and proteins. In these situations the ability to control and programme switchable surfaces will be paramount. Switchable surfaces will also find numerous applications in the field of immunosensing, where they could be used to improve the performance of biosensors, programmable DNA/protein arrays and microreactors. As in many areas of science and engineering, these developments will require a multidisciplinary ap-

proach to overcome the challenges and fully realise the exciting and wide-ranging potential of intelligent surfaces.

**Keywords:** contact angle • external stimuli • hydrophobic effect • interfaces • surface chemistry

- [1] H. Matsumoto, J. E. Colgate, *Micro Electro Mechanical Systems 1990, Proceedings: An Investigation of Micro Structures, Sensors, Actuators, Machines and Robots*, IEEE, New York, **1990**, p. 105.
- [2] J. Lee, C.-J. C. Kim, *MEMS 98, Proceedings of the 11th Annual International Workshop on Micro Electro Mechanical Systems*, IEEE, Heidelberg, **1998**, p. 538.
- [3] J. Y. Shin, N. L. Abbott, *Langmuir* **1999**, *15*, 4404.
- [4] N. L. Abbott, G. M. Whitesides, *Langmuir* **1994**, *10*, 1493.
- [5] P. Mali, N. Bhattacharjee, P. C. Searson, *Nano Lett.* **2006**, *6*, 1250.
- [6] H. Kaji, M. Hashimoto, M. Nishizawa, *Anal. Chem.* **2006**, *78*, 5469.
- [7] X. Feng, L. Feng, M. Jin, J. Zhai, L. Jiang, D. Zhu, *J. Am. Chem. Soc.* **2004**, *126*, 62.
- [8] D. E. Meyer, A. Chilkoti, *Nat. Biotechnol.* **1999**, *17*, 1112.
- [9] J. Crassous, C. Gabay, G. Liogier, B. Berge, *Proc. SPIE* **2004**, 5639, 143.
- [10] M. Vallet, B. Berge, L. Vovelle, *Polymer* **1996**, *37*, 2465.
- [11] F. Saeki, J. Baum, H. Moon, J. Y. Yoon, C. J. Kim, R. L. Garrell, *Abstr. Pap. Am. Chem. Soc.* **2001**, 222, U341.
- [12] Y.-W. Chang, D. Y. Kwok, *ICMENS 2004, Proceedings of the 2004 International Conference on MEMS, Nano and Smart Systems*, **2004**, p. 66.
- [13] H. Moon, S. K. Cho, R. L. Garrell, C.-J. C. Kim, *J. Appl. Phys.* **2002**, *92*, 4080.
- [14] P. Mach, T. Krupenkin, S. Yang, J. A. Rogers, *Appl. Phys. Lett.* **2002**, *81*, 202.
- [15] M. Vallet, M. Vallade, B. Berge, *Eur. Phys. J. B* **1999**, *11*, 583.
- [16] J. Ralston, *Aust. J. Chem.* **2005**, *58*, 644.
- [17] M. G. Pollack, R. B. Fair, A. D. Shenderov, *Appl. Phys. Lett.* **2000**, *77*, 1725.
- [18] C. Quilliet, B. Berge, *Curr. Opin. Colloid Interface Sci.* **2001**, *6*, 34.
- [19] J. Lee, C.-J. Kim in *ASME International Mechanical Engineering Congress and Exposition AES*, Nashville, **1999**, p. 397.
- [20] A. Froumkine, *Actual. Sci. Ind.* **1936**, 373, 5.
- [21] D. C. Grahame, *Chem. Rev.* **1947**, *41*, 441.
- [22] L. Minnema, H. Barneveld, P. Rinkel, *IEEE Trans. Electr. Insul.* **1980**, *15*, 461.
- [23] B. Berge, *C. R. Acad. Sci. Ser. II* **1993**, 317, 157.
- [24] W. J. J. Welters, L. G. J. Fokkink, *Langmuir* **1998**, *14*, 1535.
- [25] H. J. J. Verheijen, M. W. J. Prins, *Langmuir* **1999**, *15*, 6616.
- [26] V. Peykov, A. Quinn, J. Ralston, *Colloid Polym. Sci.* **2000**, *278*, 789.
- [27] J. Lee, H. Moon, J. Fowler, T. Schoellhammer, C. J. Kim, *Sens. Actuators A* **2002**, *95*, 259.
- [28] S. K. Cho, H. Moon, C.-J. Kim, *J. Microelectromech. Syst.* **2003**, *12*, 70.
- [29] J. S. Kuo, P. Spicar-Mihalic, I. Rodriguez, D. T. Chiu, *Langmuir* **2003**, *19*, 250.
- [30] J. Lee, C.-J. Kim, *J. Microelectromech. Syst.* **2000**, *9*, 171.
- [31] R. B. Fair, V. Srinivasan, H. Ren, P. Paik, V. K. Pamula, M. G. Pollack in *IEEE International Electron Devices Meeting (IEDM)*, IEEE, Washington, **2003**, p. 32.5.1–32.5.4.
- [32] K. Hoshino, S. Tritayprasert, K. Matsumoto, I. Shimoyama in *Proceedings of the 12th International Conference on Transducers, Solid-State Sensors, Actuators and Microsystems*, Vol. 2, IEEE, Boston, **2003**, p. 1800.
- [33] J. Hsieh, P. Mach, F. Cattaneo, S. Yang, T. Krupenkin, K. Baldwin, J. A. Rogers, *IEEE Photonics Technol. Lett.* **2003**, *15*, 81.
- [34] F. Cattaneo, K. Baldwin, S. Yang, T. Krupenkin, S. Ramachandran, J. A. Rogers, *J. Microelectromech. Syst.* **2003**, *12*, 907.
- [35] F. Mugele, J.-C. Baret, *J. Phys. Condens. Matter* **2005**, *17*, R705.
- [36] C.-Y. Chen, E. F. Fabrizio, A. Nadim, J. D. Sterling in *Proceedings of the Summer Bioengineering Conference*, Key Biscayne, Florida, **2003**, p. 1241.
- [37] M. Schneemilch, W. J. J. Welters, R. A. Hayes, J. Ralston, *Langmuir* **2000**, *16*, 2924.
- [38] B. Shapiro, H. Moon, R. Garrell, C.-J. Kim in *MEMS 03, Proceedings of the 16th Annual International Conference on Micro Electro Mechanical Systems*, IEEE, Kyoto, **2003**, p. 201.
- [39] B. Shapiro, H. Moon, R. L. Garrell, C.-J. C. Kim, *J. Appl. Phys.* **2003**, *93*, 5794.
- [40] G. Lippmann, *Ann. Chim. Phys.* **1875**, *5*, 494.
- [41] X. J. Feng, L. Jiang, *Adv. Mater.* **2006**, *18*, 3063.
- [42] L. Feng, S. Li, Y. Li, H. Li, L. Zhang, J. Zhai, Y. Song, B. Liu, L. Jiang, D. Zhu, *Adv. Mater.* **2002**, *14*, 1857.
- [43] K. K. S. Lau, J. Bico, K. B. K. Teo, M. Chhowalla, G. A. J. Amaratunga, W. I. Milne, G. H. McKinley, K. K. Gleason, *Nano Lett.* **2003**, *3*, 1701.
- [44] N. Verplanck, E. Galopin, J.-C. Camart, V. Thomy, *Nano Lett.* **2007**, *7*, 813.
- [45] J. A. M. Sondag-Huethorst, L. G. J. Fokkink, *Langmuir* **1994**, *10*, 4380.
- [46] B. S. Gallardo, V. K. Gupta, F. D. Eagerton, L. I. Jong, V. S. Craig, R. R. Shah, N. L. Abbott, *Science* **1999**, 283, 57.
- [47] C. Rosslee, N. L. Abbott, *Curr. Opin. Colloid Interface Sci.* **2000**, *5*, 81.
- [48] K. Tajima, T. Huxur, Y. Imai, I. Motoyama, A. Nakamura, M. Koshinuma, *Colloids Surf. A* **1995**, *94*, 243.
- [49] B. S. Gallardo, K. L. Metcalfe, N. L. Abbott, *Langmuir* **1996**, *12*, 4116.
- [50] N. Aydogan, B. S. Gallardo, N. L. Abbott, *Langmuir* **1999**, *15*, 722.
- [51] B. S. Gallardo, N. L. Abbott, *Langmuir* **1997**, *13*, 203.
- [52] M. Riskin, B. Basnar, V. I. Chegel, E. Katz, I. Willner, F. Shi, X. Zhang, *J. Am. Chem. Soc.* **2006**, *128*, 1253.
- [53] N. L. Abbott, C. B. Gorman, G. M. Whitesides, *Langmuir* **1995**, *11*, 16.
- [54] L. Mu, Y. Liu, S. Zhang, B. H. Liu, J. Kong, *New J. Chem.* **2005**, *29*, 847.
- [55] J. Lahann, S. Mitragotri, T.-N. Tran, H. Kaido, J. Sundaram, I. S. Choi, S. Hoffer, G. A. Somorjai, R. Langer, *Science* **2003**, 299, 371.
- [56] C. S. Tang, M. Dussweiler, S. Makohliso, M. Heuschkel, S. Sharma, B. Keller, J. Voros, *Anal. Chem.* **2006**, *78*, 711.
- [57] A. L. Hook, H. Thissen, J. P. Hayes, N. H. Voelcker, *Biosens. Bioelectron.* **2006**, *21*, 2137.
- [58] C. A. Widrig, C. Chung, M. D. Porter, *J. Electroanal. Chem. Interfacial Electrochem.* **1991**, *310*, 335.
- [59] X. Jiang, D. A. Bruzewicz, A. P. Wong, M. Piel, G. M. Whitesides, *Proc. Natl. Acad. Sci. USA* **2005**, 102, 975.
- [60] K. Ichimura, S.-K. Oh, M. Nakagawa, *Science* **2000**, 288, 1624.
- [61] G. Moller, M. Harke, H. Motschmann, D. Prescher, *Langmuir* **1998**, *14*, 4955.
- [62] C. Radüge, G. Papastavrou, D. G. Kurth, H. Motschmann, *Eur. Phys. J. E* **2003**, *10*, 103.
- [63] H. S. Blair, H. I. Pague, J. E. Riordan, *Polymer* **1980**, *21*, 1195.
- [64] L. M. Siewierski, W. J. Brittain, S. Petrash, M. D. Foster, *Langmuir* **1996**, *12*, 5838.
- [65] T. Seki, H. Sekizawa, S.-y. Morino, K. Ichimura, *J. Phys. Chem. B* **1998**, *102*, 5313.
- [66] T. Seki, H. Sekizawa, K. Ichimura, *Polym. J.* **1999**, *31*, 1079.
- [67] T. Seki, K. Tanaka, K. Ichimura, *Macromolecules* **1997**, *30*, 6401.
- [68] T. Seki, J. Kojima, K. Ichimura, *J. Phys. Chem. B* **1999**, *103*, 10338.
- [69] H. Sakai, A. Matsumura, S. Yokoyama, T. Saji, M. Abe, *J. Phys. Chem. B* **1999**, *103*, 10737.
- [70] S. Abbott, J. Ralston, G. Reynolds, R. Hayes, *Langmuir* **1999**, *15*, 8923.
- [71] M. O. Wolf, M. A. Fox, *J. Am. Chem. Soc.* **1995**, *117*, 1845.
- [72] B. C. Bunker, B. I. Kim, J. E. Houston, R. Rosario, A. A. Garcia, M. Hayes, D. Gust, S. T. Picraux, *Nano Lett.* **2003**, *3*, 1723.
- [73] R. Rosario, D. Gust, M. Hayes, F. Jahnke, J. Springer, A. A. Garcia, *Langmuir* **2002**, *18*, 8062.
- [74] R. D. Sun, A. Nakajima, A. Fujishima, T. Watanabe, K. Hashimoto, *J. Phys. Chem. B* **2001**, *105*, 1984.
- [75] J. Bico, C. Tordeux, D. Quere, *Europhys. Lett.* **2001**, *55*, 214.
- [76] J. Bico, U. Thiele, D. Quere, *Colloids Surf. A* **2002**, *206*, 41.
- [77] R. Wang, N. Sakai, A. Fujishima, T. Watanabe, K. Hashimoto, *J. Phys. Chem. B* **1999**, *103*, 2188.
- [78] I. Hiroshi, T. S. Ping, T. Shibata, K. Hashimoto, *Electrochem. Solid-State Lett.* **2005**, *8*, D23.
- [79] T. L. Sun, G. J. Wang, L. Feng, B. Q. Liu, Y. M. Ma, L. Jiang, D. B. Zhu, *Angew. Chem.* **2004**, *116*, 361; *Angew. Chem. Int. Ed.* **2004**, *43*, 357.
- [80] D. L. Huber, R. P. Manginell, M. A. Samara, B. I. Kim, B. C. Bunker, *Science* **2003**, *301*, 352.
- [81] K. F. Bohringer, *J. Micromech. Microeng.* **2003**, *13*, S1.
- [82] X.-Z. Zhang, G.-M. Sun, C. C. Chu, *Eur. Polym. J.* **2004**, *40*, 2251.
- [83] R. M. K. Ramanan, P. Chellamuthu, L. Tang, K. T. Nguyen, *Biotechnol. Prog.* **2006**, *22*, 118.
- [84] C. S. Brazel, N. A. Peppas, *Macromolecules* **1995**, *28*, 8016.

- [85] D. E. Meyer, K. Trabbic-Carlson, A. Chilkoti, *Biotechnol. Prog.* **2001**, *17*, 720.
- [86] N. Nath, A. Chilkoti, *Anal. Chem.* **2003**, *75*, 709.
- [87] J. Hyun, W. K. Lee, N. Nath, A. Chilkoti, S. Zauscher, *J. Am. Chem. Soc.* **2004**, *126*, 7330.
- [88] M. Ebara, J. M. Hoffman, A. S. Hoffman, P. S. Stayton, *Lab Chip* **2006**, *6*, 843.
- [89] M. Ebara, M. Yamato, T. Aoyagi, A. Kikuchi, K. Sakai, T. Okana, *Tissue Eng.* **2004**, *10*, 1125.
- [90] Y. Tsuda, A. Kikuchi, M. Yamato, A. Nakao, Y. Sakurai, M. Umezu, T. Okano, *Biomaterials* **2005**, *26*, 1885.
- [91] H. E. Canavan, X. Cheng, D. J. Graham, B. D. Ratner, D. G. Castner, *Langmuir* **2005**, *21*, 1949.
- [92] M. Kanzaki, M. Yamato, H. Hatakeyama, C. Kohno, J. Yang, T. Umemoto, A. Kikuchi, T. Okano, T. Onuki, *Tissue Eng.* **2006**, *12*, 1275.
- [93] J. L. Zhang, X. Y. Lu, W. H. Huang, Y. C. Han, *Macromol. Rapid Commun.* **2005**, *26*, 477.
- [94] J. Genzer, K. Efimenko, *Science* **2000**, *290*, 2130.
- [95] Y. Wang, J. X. Zheng, W. J. Brittain, S. Z. D. Cheng, *J. Polym. Sci. Polym. Chem.* **2006**, *44*, 5608.
- [96] H. Mori, A. Hirao, S. Nakahama, K. Senshu, *Macromolecules* **1994**, *27*, 4093.
- [97] S. Förster, M. Antonietti, *Adv. Mater.* **1998**, *10*, 195.
- [98] H.-Q. Xie, Y. Liu, *J. Appl. Polym. Sci.* **2001**, *80*, 903.
- [99] Y. Chen, G. Wulff, *Macromol. Chem. Phys.* **2001**, *202*, 3273.
- [100] K. Senshu, S. Yamashita, M. Ito, A. Hirao, S. Nakahama, *Langmuir* **1995**, *11*, 2293.
- [101] K. Senshu, S. Yamashita, H. Mori, M. Ito, A. Hirao, S. Nakahama, *Langmuir* **1999**, *15*, 1754.
- [102] K. Senshu, M. Kobayashi, N. Ikawa, S. Yamashita, A. Hirao, S. Nakahama, *Langmuir* **1999**, *15*, 1763.
- [103] G. Wulff, H. Schmidt, L. Zhu, *Macromol. Chem. Phys.* **1999**, *200*, 774.
- [104] K. Yamada, K. Yamaoka, M. Minoda, T. Miyamoto, *J. Polym. Sci. Polym. Chem.* **1997**, *35*, 255.
- [105] M.-P. Labeau, H. Cramail, A. Deffieux, *Macromol. Chem. Phys.* **1998**, *199*, 335.
- [106] G. Wulff, L. Zhu, H. Schmidt, *Macromolecules* **1997**, *30*, 4533.
- [107] A. Vaidya, M. K. Chaudhury, *J. Colloid Interface Sci.* **2002**, *249*, 235.
- [108] J. F. Hester, P. Banerjee, A. M. Mayes, *Macromolecules* **1999**, *32*, 1643.
- [109] T. Ishizone, K. Sugiyama, Y. Sakano, H. Mori, A. Hirao, S. Nakahama, *Polym. J.* **1999**, *31*, 983.
- [110] P. Uhlmann, L. Ionov, N. Houbenov, M. Nitschke, K. Grundke, M. Motorov, S. Minko, M. Stamm, *Prog. Org. Coat.* **2006**, *55*, 168.
- [111] S. Minko, D. Usov, E. Goreschnik, M. Stamm, *Macromol. Rapid Commun.* **2001**, *22*, 206.
- [112] X. Y. Lu, J. A. Peng, B. Y. Li, C. C. Zhang, Y. C. Han, *Macromol. Rapid Commun.* **2006**, *27*, 136.
- [113] B. Zhao, R. T. Haasch, S. MacLaren, *Polymer* **2004**, *45*, 7979.
- [114] D. Julthongpipit, Y.-H. Lin, J. Teng, E. R. Zubarev, V. V. Tsukruk, *Langmuir* **2003**, *19*, 7832.
- [115] M. C. LeMieux, Y. H. Lin, P. D. Cuong, H.-S. Ahn, E. R. Zubarev, V. V. Tsukruk, *Adv. Funct. Mater.* **2005**, *15*, 1529.
- [116] S. Minko, *Polym. Rev.* **2006**, *46*, 397.
- [117] I. Luzinov, S. Minko, V. V. Tsukruk, *Prog. Polym. Sci.* **2004**, *29*, 635.
- [118] D. Julthongpipit, Y.-H. Lin, J. Teng, E. R. Zubarev, V. V. Tsukruk, *J. Am. Chem. Soc.* **2003**, *125*, 15912.
- [119] Z. Lei, S. Bi, *J. Biotechnol.* **2007**, *128*, 112.
- [120] T. Cao, W. Yin, J. L. Armstrong, S. E. Webber, *Langmuir* **1994**, *10*, 1841.
- [121] S. H. Anastasiadis, H. Retsos, S. Pispas, N. Hadjichristidis, S. Neophytides, *Macromolecules* **2003**, *36*, 1994.
- [122] Y.-Y. Liu, X.-D. Fan, B.-R. Wei, Q.-F. Si, W.-X. Chen, L. Sun, *Int. J. Pharm.* **2006**, *308*, 205.
- [123] S. K. Thanawala, M. K. Chaudhury, *Langmuir* **2000**, *16*, 1256.
- [124] Y. Hong, S. J. Coombs, J. J. Cooper-White, M. E. Mackay, C. J. Hawker, E. Malmstrom, N. Rehnberg, *Polymer* **2000**, *41*, 7705.
- [125] I. Sendjarevic, A. J. McHugh, J. A. Orlicki, J. S. Moore, *Polym. Eng. Sci.* **2002**, *42*, 2393.
- [126] M. E. Mackay, G. Carnezini, B. B. Sauer, W. Kampert, *Langmuir* **2001**, *17*, 1708.
- [127] R. A. Bissell, E. Cordova, A. E. Kaifer, J. F. Stoddart, *Nature* **1994**, *369*, 133.
- [128] M. Gómez-López, J. A. Preece, J. F. Stoddart, *Nanotechnology* **1996**, *7*, 183.
- [129] T. Iijima, S. A. Vignon, H.-R. Tseng, T. Jarrosson, J. K. M. Sanders, F. Marchioni, M. Venturi, E. Apostoli, V. Balzani, J. F. Stoddart, *Chem. Eur. J.* **2004**, *10*, 6375.
- [130] V. Balzani, A. Credi, B. Ferrer, S. Silvi, M. Venturi in *Molecular Machines, Vol. 262. Artificial Molecular Motors and Machines: Design Principles and Prototype Systems, 1st ed.* (Ed.: K. T. Ross), Springer, Berlin, **2005**, pp. 1–27.
- [131] H. R. Tseng, D. M. Wu, N. X. L. Fang, X. Zhang, J. F. Stoddart, *ChemPhysChem* **2004**, *5*, 111.
- [132] Y. Luo, C. P. Collier, J. O. Jeppesen, K. A. Nielsen, E. Delonno, G. Ho, J. Perkins, H. R. Tseng, T. Yamamoto, J. F. Stoddart, J. R. Heath, *ChemPhysChem* **2002**, *3*, 519.
- [133] P. R. Ashton, R. Ballardini, V. Balzani, S. E. Boyd, A. Credi, M. T. Gandolfi, M. Gomez-Lopez, S. Iqbal, D. Philp, J. A. Preece, L. Prodi, H. G. Ricketts, J. F. Stoddart, M. S. Tolley, M. Venturi, A. J. P. White, D. J. Williams, *Chem. Eur. J.* **1997**, *3*, 152.
- [134] V. Balzani, *Photochem. Photobiol. Sci.* **2003**, *2*, 459.
- [135] V. Balzani, A. Credi, M. Venturi, *Pure Appl. Chem.* **2003**, *75*, 541.
- [136] E. Katz, O. Lioubashevsky, I. Willner, *J. Am. Chem. Soc.* **2004**, *126*, 15520.
- [137] V. Balzani, A. Credi, S. Silvi, M. Venturi, *Chem. Soc. Rev.* **2006**, *35*, 1135.
- [138] H. R. Tseng, S. A. Vignon, P. C. Celestre, J. Perkins, J. O. Jeppesen, A. Di Fabio, R. Ballardini, M. T. Gandolfi, M. Venturi, V. Balzani, J. F. Stoddart, *Chem. Eur. J.* **2004**, *10*, 155.
- [139] V. Balzani, A. Credi, F. M. Raymo, J. F. Stoddart, *Angew. Chem.* **2000**, *112*, 3484; *Angew. Chem. Int. Ed.* **2000**, *39*, 3348.
- [140] V. Balzani, M. Gomez-Lopez, J. F. Stoddart, *Acc. Chem. Res.* **1998**, *31*, 405.
- [141] P. R. Ashton, R. Ballardini, V. Balzani, I. Baxter, A. Credi, M. C. T. Fyfe, M. T. Gandolfi, M. Gomez-Lopez, M.-V. Martinez-Diaz, A. Piersanti, N. Spencer, J. F. Stoddart, M. Venturi, A. J. P. White, D. J. Williams, *J. Am. Chem. Soc.* **1998**, *120*, 11932.
- [142] M. Asakawa, P. R. Ashton, V. Balzani, A. Credi, C. Hamers, G. Mattersteig, M. Montalti, A. N. Shipway, N. Spencer, J. F. Stoddart, M. S. Tolley, M. Venturi, A. J. P. White, D. J. Williams, *Angew. Chem.* **1998**, *110*, 357; *Angew. Chem. Int. Ed.* **1998**, *37*, 333.
- [143] P. R. Ashton, V. Baldoni, V. Balzani, A. Credi, H. D. A. Hoffmann, M. V. Martinez-Diaz, F. M. Raymo, J. F. Stoddart, M. Venturi, *Chem. Eur. J.* **2001**, *7*, 3482.
- [144] M. Asakawa, P. R. Ashton, V. Balzani, S. E. Boyd, A. Credi, G. Mattersteig, S. Menzer, M. Montalti, F. M. Raymo, C. Ruffilli, J. F. Stoddart, M. Venturi, D. J. Williams, *Eur. J. Org. Chem.* **1999**, 985.
- [145] M. R. Diehl, D. W. Steuerman, H.-R. Tseng, S. A. Vignon, A. Star, P. C. Celestre, J. F. Stoddart, J. R. Heath, *ChemPhysChem* **2003**, *4*, 1335.
- [146] E. Ayano, C. Sakamoto, H. Kanazawa, A. Kikuchi, T. Okana, *Anal. Sci.* **2006**, *22*, 539.
- [147] J. J. Park, X. Luo, H. Yi, T. M. Valentine, G. F. Payne, W. E. Bently, R. Ghodssi, G. W. Rubloff, *Lab Chip* **2006**, *6*, 1315.
- [148] J. H. Zhou, G. Wang, J. Q. Hu, X. B. Lu, J. H. Li, *Chem. Commun.* **2006**, 4820.
- [149] E. Ayano, Y. Suzuki, M. Kanazawa, C. Sakamoto, Y. Morita-Murase, Y. Nagata, H. Kanazawa, A. Kikuchi, T. Okano, *J. Chromatogr.* **2007**, *1156*, 213.
- [150] T. P. Russell, *Science* **2002**, *297*, 964.

Received: March 30, 2007

Published online on August 27, 2007